

## 10. Michelson Interferometer (MINT) **N94-21646**

*Andrew Lacis and Barbara Carlson, NASA Goddard Institute for Space Studies*

MINT is a Michelson Interferometer designed to measure the thermal emission from the earth at high spectral resolution ( $2\text{ cm}^{-1}$ ) over a broad spectral range ( $250\text{--}1700\text{ cm}^{-1}$ ,  $6\text{--}40\text{ }\mu\text{m}$ ) with contiguous 3-pixel wide (12 mrad, 8 km field of view) along-track sampling. MINT is particularly well suited for monitoring cloud properties (cloud cover, effective temperature, optical thickness, ice/water phase, and effective particle size) both day and night, as well as tropospheric water vapor, ozone, and temperature.

The key instrument characteristics that make MINT ideally suited for decadal monitoring purposes are: (1) high wavelength-to-wavelength precision across the full IR spectrum with high spectral resolution; (2) space-proven long-term durability and calibration stability; (3) small size, low cost, low risk instrument incorporating the latest detector and electronics technology. MINT also incorporates simplicity in design and operation by utilizing passively cooled DTGS detectors and nadir viewing geometry (with target motion compensation). MINT measurement objectives, instrument characteristics, and key advantages are summarized in Table 10.1.

MINT has a well founded heritage in space-proven instrument hardware (Table 10.2) with a thoroughly demonstrated concept for information retrieval (Conrath *et al.*, 1970; Smith, 1970; Chahine, 1974; Smith and Frey, 1990). The Nimbus-3 and Nimbus-4 IRIS instruments launched in 1969/1970 obtained a one-year long climatology of high spectral resolution ( $5\text{ cm}^{-1}/2.8\text{ cm}^{-1}$ ) Earth observations over the  $5\text{--}25\text{ }\mu\text{m}$  ( $400\text{--}2000\text{ cm}^{-1}$ ) spectral range (Hanel *et al.*, 1970, 1972a; Conrath *et al.*, 1970; Kunde *et al.*, 1974). The accurate calibration and high information content of this dataset

**TABLE 10.1. Michelson Interferometer (MINT)**

### Measurement Objectives

Cloud properties: cloud cover, effective temperature, optical thickness, ice/water phase, effective particle size (all obtained day and night)

Water vapor: three levels in troposphere

Ozone: two levels in troposphere and one in stratosphere

Temperature: four levels in troposphere and surface temperature

Measurement precision required to determine interseasonal, interannual and decadal changes of all these parameters

### Instrument Characteristics

Spectral Range:  $250\text{--}1700\text{ cm}^{-1}$  ( $6\text{--}40\text{ }\mu\text{m}$ )

Spectral Resolution:  $2\text{ cm}^{-1}$

Field of View: 12 mrad (8 km) - same as EOSP

Detector:  $2\times 3$  array of uncooled deuterated triglycerine sulfate (DTGS)

Sampling: contiguous 3-pixel wide along-track sampling

### Key Advantages

Full IR spectral coverage with high resolution

High wavelength-to-wavelength precision (single detector)

Proven long-term durability and calibration stability; small size, low cost, low risk

TABLE 10.2. MINT predecessor instruments.

<u>Instrument (Spacecraft)</u>	<u>Active period</u>	<u>Spectral range (resolution)</u>	<u>Mass</u>
IRIS (Nimbus-3)	Apr 1969	400-2000 $\text{cm}^{-1}$ (5 $\text{cm}^{-1}$ )	22 kg
IRIS (Nimbus-4)	Apr 1970 - Jan 1971	400-2000 $\text{cm}^{-1}$ (2.8 $\text{cm}^{-1}$ )	22 kg
IRIS (Mariner 9)	1971	200-2000 $\text{cm}^{-1}$ (2.4 $\text{cm}^{-1}$ )	22 kg
IRIS (Voyager 1)	Sep 1977 - Aug 1981	180-2500 $\text{cm}^{-1}$ (4.3 $\text{cm}^{-1}$ )	18 kg
IRIS (Voyager 2)	Aug 1977 - 1989	180-2500 $\text{cm}^{-1}$ (4.3 $\text{cm}^{-1}$ )	18 kg
TES (Mars Observer)	Sep - Oct 1992	200-1600 $\text{cm}^{-1}$ (5 $\text{cm}^{-1}$ )	15 kg

make it a valued benchmark in climate data that only recently is beginning to be fully exploited (Prabhakara, 1988, 1990). Other predecessor instruments were the Mariner-9 IRIS launched to Mars in 1971 (Hanel *et al.*, 1972b) and the notable Voyager-1 and Voyager-2 IRIS instruments, launched on interplanetary tours in 1977, that obtained detailed information on the atmospheric structure and composition of Jupiter, Saturn, Uranus and Neptune (Hanel *et al.*, 1981, 1983; Kunde *et al.*, 1982; Conrath *et al.*, 1987, 1989; Carlson *et al.*, 1992a,b). The several IRIS instruments have been of similar mass (20 kg) and have had similar performance characteristics with respect to spectral range and resolution. All performed well in space, with the Voyager IRIS instruments operating flawlessly over a 12 year time span. The Mars Observer TES (launched in September 1992) is the most recent of IRIS type space instruments (Christensen, *et al.*, 1992). Weighing 15 kg and having a somewhat coarser spectral resolution (5  $\text{cm}^{-1}$ ), TES incorporates the latest advances in detector and electronics technology and serves as the pattern of instrument design for MINT. Thus MINT incorporates key elements that contributed to the success of predecessor instruments, but uses state-of-the art detector and electronics technology. The 8 km field-of-view of the MINT pixel, combined with its contiguous 3-pixel wide along-track sampling, is an order of magnitude improvement over the 95 km resolution of Nimbus-4 IRIS.

The infrared spectrum emitted by the earth is formed of the essentially black-body thermal emission from the earth's surface, modulated by the spectrally discreet absorption and re-emission due to atmospheric gases and by the spectrally smoother variations in absorption, emission and scattering by clouds. As a result the outgoing thermal spectrum contains detailed information on the concentration and vertical distribution of atmospheric gases, cloud properties (including effective particle size and optical thickness), as well as the surface and atmospheric temperature structure. The prominent spectral features that appear in the clear sky thermal spectrum (Fig. 10.1) are the 15  $\mu\text{m}$   $\text{CO}_2$  band used primarily for temperature sounding, the 9.6  $\mu\text{m}$  ozone band, and the 7 to 8  $\mu\text{m}$   $\text{CH}_4$  and  $\text{N}_2\text{O}$  complex. Water vapor absorption spans the entire spectrum, being strongest for wavelengths less than 7  $\mu\text{m}$  and greater than 20  $\mu\text{m}$ . The relatively clear window region from 8 to 12  $\mu\text{m}$  contains information on tropospheric water vapor distribution and is also the region where the spectral signature of clouds is most apparent.

At each wavelength, the radiation emerging at the top of the atmosphere contains contributions that originate from different levels of the atmosphere. These contribution functions (Fig. 10.2) are determined by the atmospheric vertical distribution of the absorber, absorption coefficient strengths, and atmospheric temperature profile. For  $\text{CO}_2$ , since the absorber distribution and absorption coefficients are known, the contribution functions permit retrieval of the atmospheric temperature profile. With the temperature profile determined, the contribution functions are used to obtain information on the atmospheric concentration and vertical distribution of water vapor and ozone.

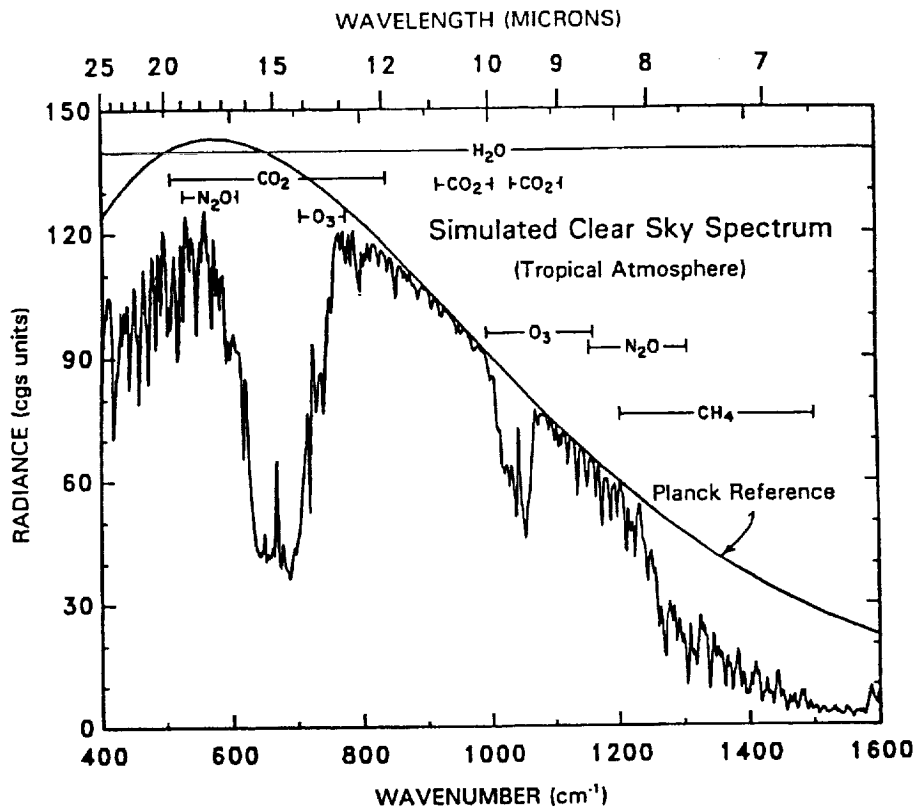


Fig. 10.1. Clear sky spectrum at 3 cm<sup>-1</sup> (IRIS) resolution. The spectral locations of the principal absorption features are identified.

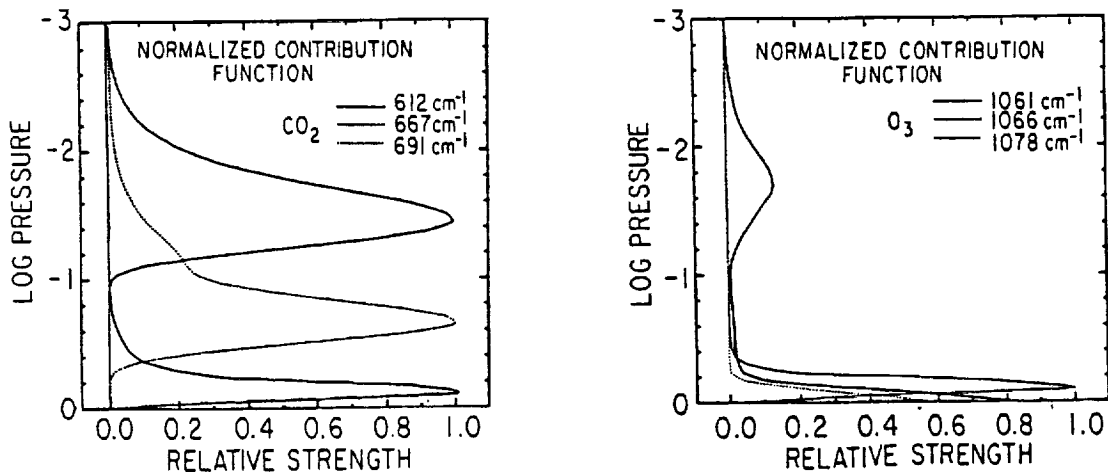


Fig. 10.2. Contribution (weighting) functions illustrating height and wavelength dependence of radiance emission level used in retrieval of height dependent profiles for temperature from the CO<sub>2</sub> band (left) and ozone (right).

Each atmospheric constituent has a unique spectral signature that can be used to determine its atmospheric concentration and location. Furthermore, this spectral signature is spread over hundreds of wavelength points in the measured spectrum and is very strongly correlated in wavelength space. Instrumental noise, on the other hand, is uncorrelated, thus permitting unambiguous statistical extraction of small changes in absorber distribution that are not readily measurable with a discreet channel instrument. The capability for precise long-term monitoring of atmospheric constituents with MINT is tied to the very high wavelength-to-wavelength precision that is only possible with an interferometer type instrument. In the following, we illustrate the retrieval capabilities for MINT by using simulated Nimbus-4 IRIS spectra, since the spectral resolution, range, and instrumental noise characteristics are similar for the two instruments.

The spectral signature of clouds is formed by contributions of upwelling thermal radiation that is transmitted through the cloud, by thermal radiation emitted by the cloud, and to lesser extent, by the reflection of downwelling radiation that is incident on the cloud. Thus the cloud spectral signature is determined by the spectral dependence of the cloud radiative properties as well as the cloud and underlying temperature structure, which in the window region is essentially the surface temperature. Since the cloud radiative properties depend directly on the refractive indices of water and ice, the effective cloud particle size, and the cloud optical thickness, the measured infrared spectrum can be used to retrieve cloud liquid/ice phase, particle size and optical depth, including also the effective cloud temperature. Within the 8 to 12  $\mu\text{m}$  window region, clear sky spectra conform closely to the Planck spectral distribution. Thus clouds are detected and identified by their degree of departure from a Planck spectrum.

Liou *et al.* (1990) and others have shown that cirrus cloud properties can be derived from thermal infrared spectra. As shown in Fig. 10.3, the retrieval of cirrus cloud optical thickness information with MINT is possible over a broad dynamic range. A cirrus cloud of optical thickness  $\tau = 0.1$  is easily differentiated from the clear sky spectrum across a broad range of wavelengths, indicating that much smaller optical thickness would be detectable with data accumulation and statistical analysis. MINT can also discriminate among optical thicknesses as large as  $\tau = 5$  to 10. This is because the diffusely transmitted radiation persists for relatively large optical thicknesses even though the direct emission from the cloud becomes saturated at smaller optical depths. Similar behavior is exhibited by water clouds, but due to differences in the spectral dependence of refractive indices, the spectral signature of water clouds shows characteristic spectral differences that permit phase discrimination.

Besides optical depth, the cloud spectral signature is also strongly dependent on particle size. This is illustrated in Fig. 10.4 for a typical water cloud of optical depth  $\tau = 5$ , for effective particle sizes of 5, 10, and 30  $\mu\text{m}$ . The difference spectra in the lower portion of the figure show the relative changes in radiance for clouds of 5 and 30  $\mu\text{m}$  particles with respect to the 10  $\mu\text{m}$  particle cloud spectrum. The particle size spectral signature becomes more pronounced toward smaller particle sizes, while for very large particles the spectrum becomes more Planck-like in character. The estimated accuracy of effective particle size retrieval of a water cloud is about 5 percent, thus 0.5  $\mu\text{m}$  for 10  $\mu\text{m}$  particles.

Relative cloud height changes of order 5 to 10 mb can also be detected in a single comparison of two spectra. The spectral signature for a 10 mb cloud height change is shown in the lower portion of Fig. 10.5 for a cirrus cloud of optical thickness  $\tau = 1$ . Averaging over many spectra would reduce the uncorrelated noise component relative to the spectral signature and allow a cloud height accuracy of the order of 1 mb for seasonal-mean cloud height determination.

MINT sensitivity to changes in atmospheric water vapor distribution is shown in Fig. 10.6. Here, the upper tropospheric water vapor between 300-700 mb is increased by 10 and 20 percent and the spectral differences compared to a standard reference profile. While the spectral signature of

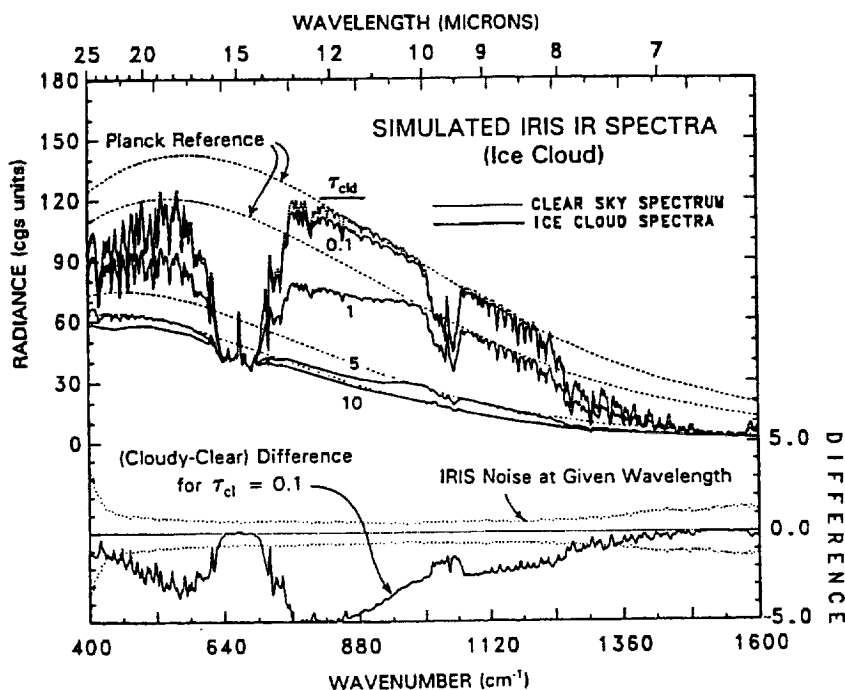


Fig. 10.3. Optical depth dependent spectral signatures of ice clouds. The difference spectrum between clear sky and optically thin ( $\tau = 0.1$ ) ice cloud in the lower portion of the figure shows that MINT will detect sub-visible cirrus.

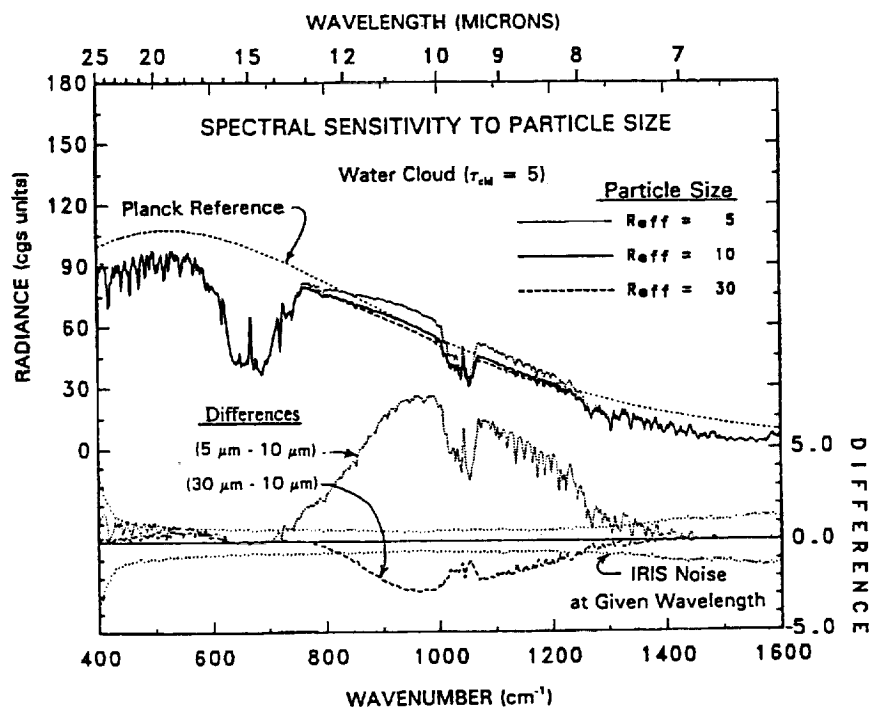
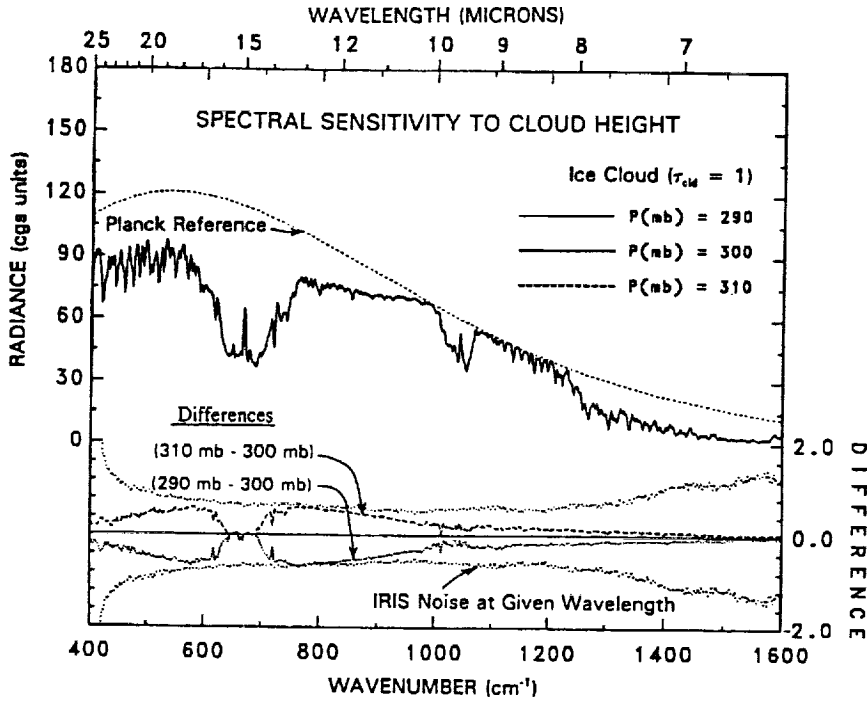
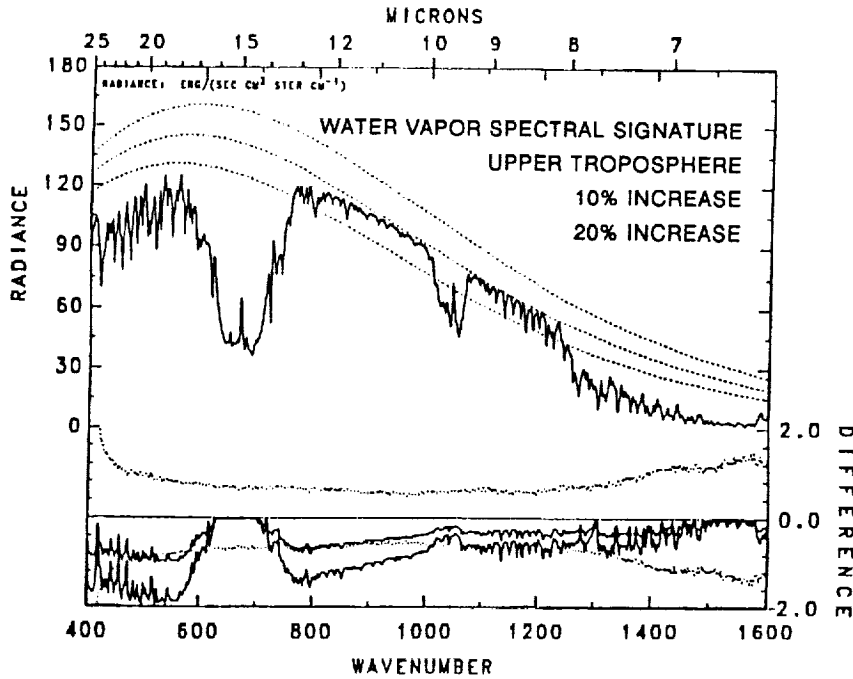


Fig. 10.4. Spectral sensitivity to particle size variations in a water cloud. The difference spectra in the lower portion of the figure shows the feasibility of MINT retrieval of cloud particle size.



**Fig. 10.5.** Spectral sensitivity to cloud height variations. The difference spectrum in the lower portion of the figure shows that 10 mb cloud-height variations are detectable within the noise level of a single IRIS measurement. The performance of mint will be similar but with higher spatial resolution.



**Fig. 10.6.** Spectral sensitivity to changes in tropospheric water vapor amount. The difference spectra in the bottom of the figure demonstrate that a 10% change in upper tropospheric water vapor will be detectable in a single MINT measurement.

water vapor is spread across the entire spectrum, the 10 percent water vapor increase in the upper troposphere produces a barely noticeable (less than 1 percent) reduction in absolute radiance at any one wavelength. To reliably detect this change with standard channel-instrument technology would require unrealistic precision and calibration. However, as shown on an expanded scale in the difference spectrum at the bottom of the figure, this change in water vapor is clearly detectable through a single comparison of two clear-sky spectra because, in effect, the signals of all wavelengths are combined to produce a different spectrum shape. Sensitivity to atmospheric location of the water vapor change is also contained in the spectral signature. For example, the spectral change near  $20 \mu\text{m}$  ( $400\text{--}600 \text{ cm}^{-1}$ ) that is so prominent for upper tropospheric water vapor, is virtually absent for water vapor changes near the ground. Furthermore, the differential sensitivity at the low and high frequency wings of the  $15 \mu\text{m}$   $\text{CO}_2$  band to overlapping water vapor absorption (Ackerman, 1979; Clough *et al.*, 1989a) provides more independent observational constraints on the retrieval of temperature and water vapor profiles than is possible using measurements of only the high frequency wing. In similar fashion, spectral differences measured within the  $9.6 \mu\text{m}$  ozone band are used to detect changes in tropospheric and stratospheric ozone amount. The known variation of water and ozone absorption with wavelength allows separation of atmospheric and surface effects, which allows MINT to obtain much better measurements of surface temperature and emissivity than possible with discrete channel instruments.

The estimated accuracies of MINT data products are summarized in Table 10.3. Because the spectral signatures of the measured quantities (e.g., effective cloud particle size, phase, optical thickness, atmospheric and surface temperature, water vapor, ozone) are accurately known, they can be statistically extracted from the measurement noise. Thus errors representative of single "pixel" retrievals can be significantly reduced by averaging multiple views of the same and nearby regions, or obtaining monthly and seasonal averages. As is the case for EOSP, the accuracies obtainable with MINT are generally higher than with current operational satellite instruments, which is attributable to the high wavelength-to-wavelength precision of the MINT measurements. The accuracy of the MINT retrievals can be further improved through greater averaging. Moreover, because of the high degree of calibration stability of MINT (demonstrated by its predecessors) the simultaneous measurements by MINT instruments on two satellites permits acquisition of a homogeneous calibrated climatology of MINT data products on decadal time scales. A summary of our error estimates for all the parameters, and a comparison with the requirements, is given in Table 7.4.

**TABLE 10.3. Estimated MINT data product accuracies.**

	Single Field of View	Monthly 500 km Mean
<b>Clouds</b>		
Effective Temperature	1-2K	< 1K
Optical Thickness	12%	5%
Particle Size	9%	5%
Phase (confidence)	99%	99%
<b>Water Vapor</b>		
300-700 mb	10%	5%
700-1000 mb	< 10%	< 5%
<b>Ozone</b>		
Tropospheric Mean	15%	< 10%
Stratospheric Mean	10%	< 5%